Improvements of Droplet Size Distribution Measurements with the Fast-FSSP (Forward Scattering Spectrometer Probe)

JEAN-LOUIS BRENGUIER* AND THIERRY BOURRIANNE

Météo-France, CNRM/GMEI, Toulouse, France

AFRANIO DE ARAUJO COELHO+

Cloud Physics Laboratory, Federal University of Ceara, Fortaleza, Ceara, Brazil

JACQUES ISBERT

ONERA-CERT (DERO), Toulouse, France

ROBERT PEYTAVI AND DOMINIQUE TREVARIN

Météo-France, CNRM/GMEI, Toulouse, France

PERRY WESCHLER

Department of Atmospheric Science, University of Wyoming, Laramie, Wyoming

(Manuscript received 24 April 1997, in final form 24 September 1997)

ABSTRACT

The basics of single particle measurements are discussed and illustrated with measurements of the droplet size distribution with an optical spectrometer, the Forward Scattering Spectrometer Probe (FSSP), and its improved version, the Fast-FSSP. The various sources of uncertainties are successively analyzed: the statistical significance of an incomplete sampling of the particle population, counting losses due to coincidence of particles and electronic dead time of the counter, artificial broadening of the size distributions by the coincidences, inhomogeneities of the sensitive volume of the probe, ambiguities of the Mie scattering curve, errors on the sampled volume, and, finally, the uncertainties on the size calibration of the instrument. It is demonstrated with examples of data collected with the Fast-FSSP that additional parameters, such as the pulse duration and the interarrival times between detections, are crucial for improving the sizing of the particles and the retrieval of the spatial evolution of the size distribution at the smallest scales.

1. Introduction

Particle measurement is a large but very specific field in experimental physics that refers to the characterization of populations of solid or liquid particles suspended in a gas or liquid. Characterization means the measurement of the frequency distributions of size, mass, chemical composition, or any other physical or chemical property of the particles. Various instruments are available for such measurements. They can be classified in two types: integrators and single particle counters (SPCs). An integrator samples a large number of particles simultaneously and measures the sum of the contributions from each particle. For example, a nephelometer is an optical integrator that measures the light scattered by a particle population along various directions. Some characteristics of the particle population, such as the distribution of sizes or refractive indices, can then be retrieved by inversion of the scattering integral over the particle population.

On the contrary, an SPC detects particles individually and directly measures the particle characteristics. The distribution is obtained only after many particles have been measured. Both types of instruments can be used for sampling a particle population, but the sources of uncertainties are quite different. This paper addresses the basics of single particle counting, the sources of

* Additional affiliation: National Center for Atmospheric Research/ATD+MMM, Boulder, Colorado.
+ Additional affiliation: CNRM/GMEI, Toulouse, France.

Corresponding author address: Dr. Jean-Louis Brenguier, Météo-France, CNRM/GMEI/MNP, 42 av. Coriolis, 31057 Toulouse, Cedex 01, France.
E-mail: jlb@meteo.fr

uncertainties, and the available hardware and software solutions for improving the measurements. There is a large variety of studies published about SPCs in the field of nuclear physics or aerosols, for example. In this paper, the discussion is focused more specifically on airborne measurements of cloud particles and is illustrated with measurements made with the Forward Scattering Spectrometer Probe (FSSP-100) and its improved version, the Fast-FSSP. Detailed information about the FSSP can be found in Dye and Baumgardner (1984), Baumgardner et al. (1985), Brenguier (1989), and Baumgardner and Spowart (1990).

2. Single particle counting

Since particles are suspended in a continuous medium—gas or liquid—the distributions are generally expressed in terms of volumetric or specific concentrations, that is, the number of particles per unit volume or unit mass of medium. The continuous measure of particle characteristics is sampled in classes resulting in a series of concentrations per interval of the measured parameter or a histogram. In this paper, we consider the case of droplet size measurements. Therefore, we will refer to size histograms (cm^{-3}) or to size distributions ($cm^{-3}\ \mu m^{-1}$), after dividing each concentration by the class width. This last measure is directly comparable to the continuous size distribution, $f(\phi)d\phi$, used in microphysical models. However, the following discussion can be extrapolated, unless specified, to any other particle property, such as mass or chemical composition.

To build a histogram, a large number of particles are needed. Therefore, a significant volume $V_s = Sv_pT_s$ of the gas containing the particles must be sampled during a time period T_s, where S is the sampling section of the counter and v_p is the particle velocity through that section. Thus, Sv_p is the rate of sampling volume of the counter. The histogram is derived as

$$C_{[\phi_i,\phi_{i+1}]}(V_s) = \frac{N_{[\phi_i,\phi_{i+1}]}(T_s)}{V_s} = \frac{T_s \times \overline{\lambda}_{[\phi_i,\phi_{i+1}]}(T_s)}{V_s}, \quad (1)$$

where $C_{[\phi_i,\phi_{i+1}]}(V_s)$ is the concentration of droplets with sizes between ϕ_i and ϕ_{i+1} in the volume V_s; $N_{[\phi_i,\phi_{i+1}]}(T_s)$ is the number of particles with sizes between ϕ_i and ϕ_{i+1}, sampled in the volume V_s; and $\overline{\lambda}_{[\phi_i,\phi_{i+1}]}(T_s) = N_{[\phi_i,\phi_{i+1}]}/T_s$ is the mean counting rate of droplets with sizes between ϕ_i and ϕ_{i+1} during the sampling period T_s. When $[\phi_i, \phi_{i+1}]$ corresponds to the whole diameter range of the probe, C is referred to as the total droplet concentration. When $[\phi_i, \phi_{i+1}]$ represents a size class of the instrument, the mean droplet density in the class is derived as $\overline{f}_i = C_i/(\phi_{i+1} - \phi_i)$ and the series of the $\overline{f}_i$ values form the droplet size distribution.

It must be emphasized that in most cases it is unrealistic to sample the whole particle population. Therefore, the distribution derived from a limited sample is only an estimation of the actual distribution, and its statistical significance must be considered. This subject will be discussed briefly at the beginning of section 4. Assuming then that the particle sample is statistically significant, we will identify the various sources of uncertainty in the calculation of the droplet size distribution: coincidence and dead time losses in section 4a, particle missizing in section 4b, errors on the sampled volume in section 4c, and, finally, uncertainties due to the probe calibration in section 4d. For each case, we will explain how the specific uncertainties have been reduced by improving the optics and electronics in the Fast-FSSP. The following section is devoted to a short description of the FSSP and the modifications made in the design of the Fast-FSSP.

3. The main characteristics of the standard and Fast-FSSP

The FSSP manufactured by Particle Measuring Systems (Boulder, Colorado) is a single particle counter for airborne droplet measurements in clouds. The Fast-FSSP is a modified version that has been developed at Météo-France. In the probe's sampling tube, a thin laser beam is exposed to the airflow. The beam is then masked by a dump spot. When a droplet crosses the beam, the light scattered forward around the dump spot (between 3° and 12°) is collected by detection diodes. The main diode (*signal*) is used for the determination of the droplet size (the amplitude of the pulse is nearly proportional to the square of the diameter). The second diode (*annulus* in the standard probe, *slit* in the Fast-FSSP) provides information about the location of the droplet trajectory across the laser beam.

In the standard probe, the annulus diode allows selection of a cylindrical portion of the beam, which is called the depth of field (DOF), at the middle of the sampling tube and centered at the focal point of the beam, where the intensity of the laser is maximum [see Figs. 1 and 2 in Dye and Baumgardner (1984)]. Both the signal and annulus pulses are processed by analog electronics, and their amplitudes are compared for DOF selection. An additional test is then needed for rejecting particles crossing the beam inside the DOF but at the beam edge. This second selection (velocity rejection) is performed by comparing each pulse duration to the mean pulse duration. Only pulses longer than the mean are accepted. The probe then sends a strobe to the acquisition system each time a detection is valid with respect to the DOF and beam edge selections. For each strobe, the acquisition system records the pulse amplitude for droplet sizing, coded on 4 bits (15 size classes), corresponding to a diameter range selectable from the following: 0.5–8, 1–16, 2–32, or 2–47 μm. In addition, the probe provides a count for all particles valid in the DOF (total strobe) and for all the detections (total reset). In a standard FSSP, about 20% of the detections are

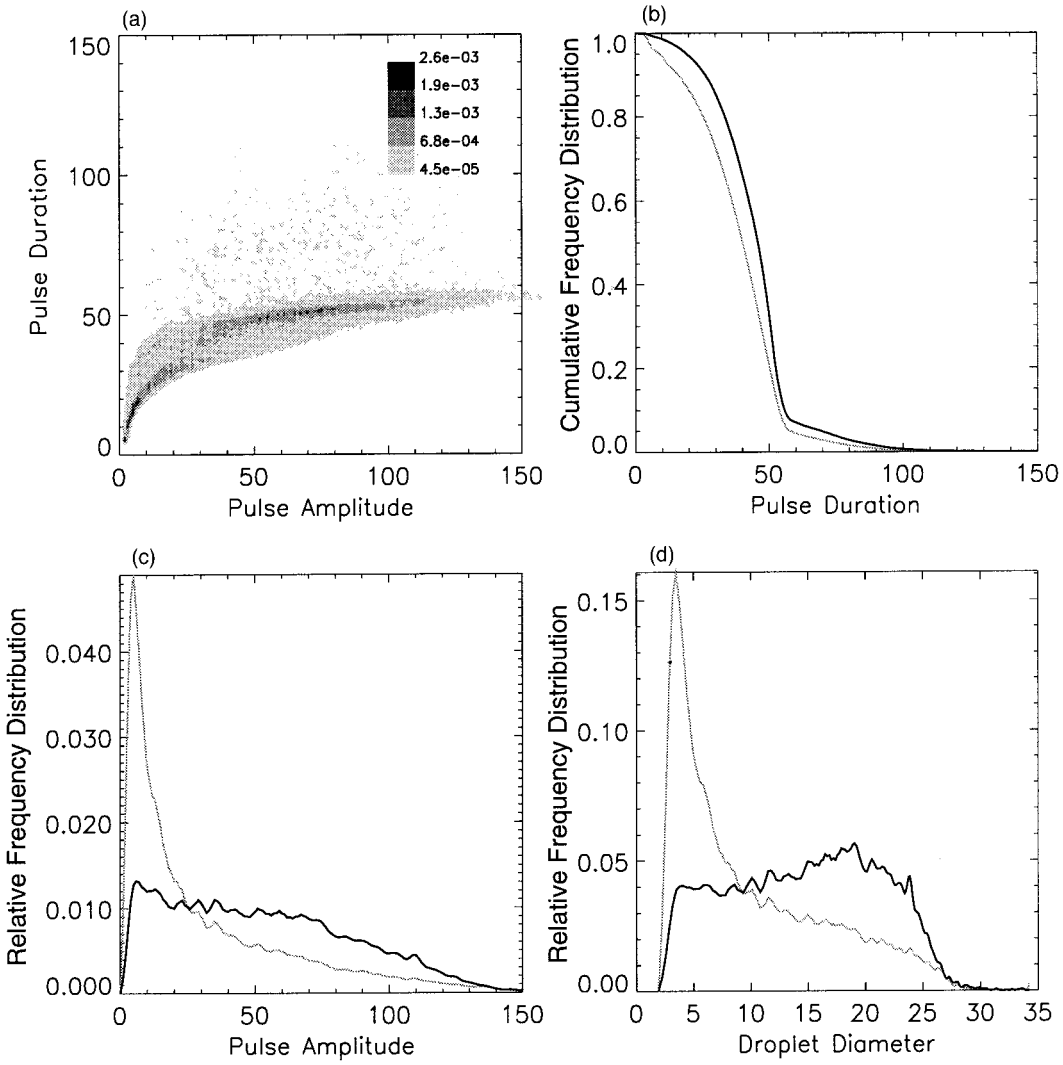

FIG. 1. Fast-FSSP data (standard optics) collected in nonprecipitating cumulus during the SEMAPHORE-93 experiment in the Azores region. Merlin flight 93-27, 1459:12–1459:16 UTC 11 October. (a) Matrix of the conditional frequency distribution of pulse duration vs pulse amplitude for DOF-accepted counts. The unit in pulse duration is 1/16 μs; the unit in pulse amplitude is 1/256 of the maximum voltage produced by a droplet of about 45 μm. Voltages and droplet diameters are not linearly dependent. The dashed horizontal line corresponds to the mean pulse duration (44 digits or 2.75 μs). (b) Cumulative frequency distribution of pulse duration for all the detections (thin line) and only the DOF-accepted counts (thick line). (c) Frequency distribution of pulse amplitude for total counts (thin line) and the DOF-accepted counts (thick line). (d) Size distribution (μm^{-1}) derived from total counts (thin line) and DOF-accepted counts (thick line).

accepted in the DOF (total strobe/total reset ≈20%) and only 50% (62% theoretically) of the DOF-accepted detections are valid after rejection of the beam edge detections (sum of accepted counts/total strobe ≈50%). Thus, all together, only 10% of the detections are usable for sizing.

The ratio of usable to total detections is crucial for any SPC. In fact, since the sensitive volume is finite, there is always a probability that some particles will cross the volume at the edge and be poorly characterized. The problem is even more severe if the volume is not uniform (the intensity of the incident light in an optical counter, for example), so that only a limited portion of the volume is usable for sizing. There is a possibility of statistically correcting the resulting broadening of the measured distributions, but it is also efficient to select a priori the particles crossing in the most uniform region of the beam volume, as in the FSSP. There is also a strong constraint on the ratio of usable volume to total sensitive volume, which will be discussed in section 4c.

In the Fast-FSSP, the slit diode (similar to the system used in the FSSP-300) allows the selection of a limited portion of the beam located at the focal point and along

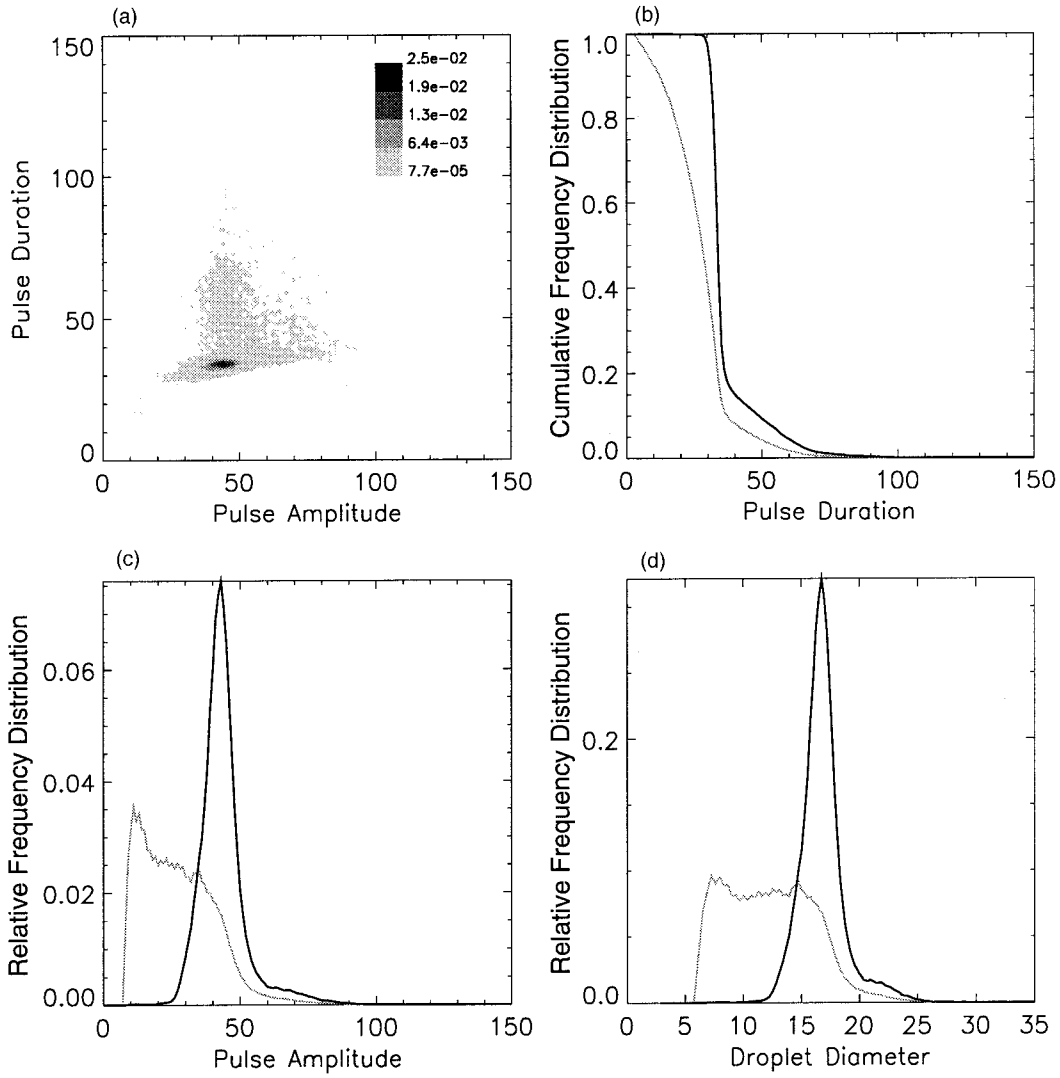

FIG. 2. Same as Fig. 1 for Fast-FSSP data (new optics) collected in a nonprecipitating cumulus during the SCMS-95 experiment in the Cape Canaveral, Florida, region. Merlin flight 95-11, 1631:40–16:31:44 UTC 10 August.

the beam axis so that the beam edge selection is no longer needed [see Fig. 2 in Baumgardner et al. (1992)]. Both signal and slit pulses are then converted from analog to digital at a 16-MHz rate on 8 bits (255 size classes). For each detection, the probe provides the acquisition system with a strobe, the amplitude of the pulse on 8 bits, its duration on 8 bits, the interarrival time between the detections (14 bits), and the validation flag for the DOF.

The amount of data produced by the Fast-FSSP and its acquisition system (up to 500 kbytes s^{-1}), which records these parameters for each detected droplet, is, of course, much larger than for the FSSP with a standard acquisition system. However, it will be demonstrated throughout this paper that these data are complementary and extremely useful for improving the accuracy of the measurements.

4. Uncertainties in the measurement of the droplet spectrum

Airborne measurements of particles in clouds are particular in the sense that a sampling cannot be repeated as in the laboratory; most of the cloud microphysical characteristics are changing during the time needed for an aircraft to repeat a cloud penetration. Therefore, each sample is a unique realization of a random nonstationary Poisson process (Pawlowska et al. 1997). If particles are counted over a fixed sampling period, as with most of the acquisition systems, the statistical significance of a sample increases with the number of counted particles. For example, $N = 1000$ particles must be counted in each class for the standard deviation to be smaller than 3%. However, during the counting, the aircraft is moving through the cloud. Therefore, a compromise must

be chosen between the significance of the estimation and the spatial–time resolution of the measurements.

Pawlowska et al. (1997) have developed an original approach based on optimal estimation. When the statistics of the counting process is known, a Poisson type in this case, optimal estimation provides a way of 1) prescribing explicitly a model for the statistics of the process driving the evolution of the distributions and 2) deriving the probability density function of the particle concentration from the unique measured series of particle arrival times in the counter. Such an approach is significantly more consuming in computer time than the current method, but it considerably improves the amount of information that can be derived from particle measurements.

Details about optimal estimation applied to droplet measurements are given in Pawlowska et al. (1997), but the most important thing to note here is that such processing techniques are usable only when the complete series of interarrival times are available. The primary improvement in designing the Fast-FSSP has been the elimination of the electronic dead time of the standard probe. In the standard version, each pulse (about 2-μs duration) is followed by a delay (6 μs if the pulse has been generated by a particle in the DOF, 2 μs otherwise) during which the probe is unable to detect a new particle. The interarrival time can be measured only between interrupts following the delays, and the measured interval includes the pulse and the delay durations. This delay is fixed and its effects can be taken into account in the processing method, but the pulse duration is variable and its effects cannot be corrected. In the Fast-FSSP, there is no dead time since the pulse duration and interarrival time are sampled at 16 MHz and each value is recorded for providing an unbiased series of interarrival times. For example, with a counting rate of about 50 000 s^{-1}, typical of a droplet concentration of 250 cm^{-3}, a satisfactory estimation of the concentration can be obtained with a time resolution of 1 ms, while standard processing cannot be applied at a frequency higher than 50 Hz (see Fig. 7).

Statistical significance is a critical source of errors that has often been neglected. For example, calculations of the cloud liquid water content (LWC) from droplet size measurements are strongly affected by random variations in the counting of big droplets because only a few of these droplets contain a significant portion of the LWC. The second type of errors can now be addressed by assuming that the measured sample is statistically significant. The sources of uncertainties will be identified and successively discussed in the following subsections in order to show how the additional parameters provided by the Fast-FSSP are used to improve this measurement.

a. Uncertainties in particle counting (N_i)

For simplicity, the errors in N_i may be addressed in two steps. First, one may consider only the estimation of the total droplet concentration, in the diameter range of the instrument (this section). Missizing of the particles can be addressed in a second step (section 4b). Thus, when two (or more) particles are present simultaneoulsy in the sensitive volume, the SPC can detect only one particle, and the counted number is always smaller or equal to the actual number of particles crossing the sensitive volume. If there is a dead time, as in the standard probe, additional particles can be lost if they cross the sensitive volume during the dead time. While coincidence events are inherent to any SPC because the sensitive volume of the counter is finite, the dead time can be significantly reduced. In the Fast-FSSP, the dead time is negligible (equal to one period of the digital sampling, 1/16 μs).

The coincidence problem has been largely discussed in the past, and a review of the various correcting methods is given in Brenguier et al. (1994). In summary, the actual number of particles can be derived from measurements of the counted rate and the activity or sum of pulse durations during the sampling period [Brenguier et al. (1994), section 2c(1)]. It can also be derived from the measured series of interarrival times as the slope of their cumulative frequency distribution (in log scale) or by the compensation method [Brenguier et al. 1994, section 2c(2)].

Measurements of the parameters needed for the correction have been significantly improved with the Fast-FSSP, and the estimation of the actual particle rate through the counter is more accurate. Brenguier (1993) shows that even at very high droplet concentrations up to 2000 cm^{-3} the two independent techniques for deriving the actual rate (coincidence equation and interarrival times) agree to within 5% with Fast-FSSP data, while at such a concentration the uncertainty on the estimation of the coincidence correction can be of the order of 50%–100% with the standard probe, where activity is not accurately measured (Brenguier 1989).

More generally the conclusions for improving measurements of the particle rate with an SPC are as follows.

- As long as the probability of coincidence is negligible, counting the particles provides an accurate estimation of the actual particle rate λ through the counter.
- At larger concentrations, the measurement of the counter activity significantly improves the calculation of the correction factor. The activity is measured by cumulating the pulse durations (and the delays in the standard probe) during the sampling period. It is thus crucial to accurately measure each pulse duration (and delay) with a resolution better than one-tenth of its mean duration (1/4 to 1/10 in the standard FSSP, 1/32 in the Fast-FSSP) and to use a perfectly symmetrical clock; otherwise, small errors on each pulse duration are not statistically compensated and the measured activity is biased (Brenguier 1989; Coelho 1996).
- The frequency distribution of the interarrival times between detections provides an independent estima-

tion of the actual rate, which is not affected by coincidences (Baumgardner 1986; Baumgardner et al. 1993). It is preferable to measure time intervals that do not include pulse durations since their random variability affects the frequency distribution of interarrival times. Since more than 63% of the interarrival times are shorter than $1/\lambda$, it is also recommended to sample time intervals with a resolution better than $1/10\lambda$.

b. *Uncertainties in particle sizing (ϕ_i)*

After detection, each particle is sorted according to its size. However, some particles are not classified correctly. Generally, particles of a given size are sorted in their nominal size class and partially in the adjacent classes. This phenomenon is referred to as artificial spectral broadening. Examples of spectral broadening and the correction methods have been discussed by Cooper (1988), Baumgardner and Spowart (1990), Kim and Boatman (1990), and Wendish et al. (1996). We will show two examples of data collected with the Fast-FSSP to illustrate the efficiency of the new optics for the DOF selection and the potential of an additional measured parameter, the pulse duration, for sizing validation.

1) EXAMPLES OF DATA COLLECTED WITH THE FAST-FSSP

Figures 1 and 2 show the conditional frequency distribution of the measured amplitude versus pulse duration [panel (a)], the cumulative frequency distribution of the measured pulse durations [panel (b)], the frequency distribution of the measured amplitudes [panel (c)], and the corresponding size distributions [panel (d)]. In Figs. 1a and 2a the distribution has been derived only with DOF-accepted counts. In Figs. 1 and 2 [panels (b), (c), and (d)], the thin line corresponds to all the detections, and the thick line to only DOF-accepted counts. Both cases correspond to spectra measured in small nonprecipitating cumuli. The data presented in Fig. 1 have been collected over the Atlantic Ocean (Azores region) during the SEMAPHORE experiment (Eymard et al. 1996) in 1993. The Fast-FSSP was still equipped with the standard FSSP-100 optics. The data presented in Fig. 2 have been collected in Florida (Cape Canaveral region) during the SCMS experiment in 1995 (flight me9511 on 10 August). The Fast-FSSP was then equipped with the new optics.

Figure 1 illustrates precisely the result of the DOF selection in a standard FSSP. Note from Fig. 1c that the proportion of small amplitudes is significantly reduced after DOF selection. This fact demonstrates that particles crossing the beam far from the focal point, in regions of reduced incident light intensity, are correctly rejected. However, the DOF amplitude distribution is still broad and so is the size spectrum (section 1d). Figure 1a shows that the small amplitudes correspond to short pulse durations from particles crossing the beam edge in the DOF. This statement is corroborated by Fig. 1b that shows a distribution typical of particles crossing a cylindrical beam: $P(T) = [1 - (T/T_M)^2]^{1/2}$, where $P(T)$ is the cumulative distribution for the duration to be smaller than T, and T_M is the maximum pulse duration, when a particle crosses the beam axis.

In the standard probe, only pulses with durations larger than the mean duration in the DOF are accepted by the velocity criterion. In this case, the mean duration is equal to 44 (2.75 μs). Figure 1a shows that the pulse duration on average increases slightly with the pulse amplitude. In addition, the mean pulse duration is biased by the long pulses of coincident particles. Therefore, the percentage of accepted counts is lower for small droplets with small amplitudes than for the big ones, and the spectral shape is distorted.

The effects of coincidences are also noticeable in Fig. 1a, where some values of pulse duration are much larger than the maximum for single droplets. This effect is represented in Fig. 1b by the tail in the distribution for durations longer than 55. The shape of this distribution has been modeled by Brenguier and Amodei [1989, Eq. (A11)]. In particular, Brenguier (1989, section 4b) has shown that the mean pulse duration is biased by these long pulses of coincident particles and so is the percentage of velocity accepted counts that decreases when the rate of coincidence increases.

Figure 2 shows a spectrum of small droplets sampled with the new optics. Despite the fact that the clouds sampled in Figs. 1 and 2 were not similar and directly comparable, the difference between Figs. 1b and 2b is significant. The comparison shows that the distributions of pulse durations for all the detections (thin line) are similar for the standard and the new optics (cylindrical beam). On the contrary, the distributions for DOF-accepted particles (thick line) are quite different. With the new optics (Fig. 1b), the distribution is sharp with 80% of the values between 30 and 35. This is typical of particles crossing the beam close to its axis. Coincidence effects are still noticeable, but particles crossing the beam edge have been optically rejected. The resulting spectrum is thus particularly narrow, and additional selection is no longer needed. These two figures will be further discussed in the next sections.

2) SPECTRAL BROADENING CORRECTIONS

The general method for correcting spectral broadening has been applied to the FSSP by Cooper (1988). It consists in the determination of the transfer matrix of the probe, which is defined as follows.

The diameter scale is discretized in n classes. The actual size distribution is represented by the discrete spectrum or vector $\mathbf{f}_a$ of dimension n. The measured spectrum is represented by the vector $\mathbf{f}_m$ of dimension n. The transfer matrix $\mathbf{P}(i, j)$ of dimension $n \times n$ is made of the probabilities for a particle of size i to be counted in the class j, so that

$$\mathbf{f}_m = \mathbf{P}(i, j)\mathbf{f}_a. \quad (2)$$

Once the matrix $\mathbf{P}$ has been determined, the actual spectrum can be retrieved from any measured spectrum by an inversion of Eq. (2). The method has been used by Baumgardner and Spowart (1990), Kim and Boatman (1990), and Wendisch et al. (1996) for correcting the spectral broadening due to the time response of the electronics and the inhomogeneities of the laser beam in the standard probe. Cooper (1988) considered a more complicated process—that is, the effects of coincidences on the spectral shape. In this case, Eq. (2) is more difficult to invert because it is nonlinear in $\mathbf{f}_a$. The main limitation of the method is that the transfer matrix is ill conditioned so that additional constraints on the shape of the spectrum are needed.

The main improvements with the Fast-FSSP are a better size resolution (255 size classes instead of 15, for the same diameter range) and the recording of the pulse duration for each detection. The measured spectrum is no longer a one-dimensional vector of the frequency distribution of sizes (or pulse amplitudes) but rather a matrix $\mathbf{M}(A_j, T_k)$ of the conditional frequency distribution of the measured amplitude A_j versus pulse duration T_k (255 classes, from 1/16 to 16 μs). The transfer equation becomes

$$\mathbf{M}(A_j, T_k) = \sum_{i=1}^{n} \mathbf{P}(\phi_i, A_j, T_k)\mathbf{f}_a(\phi_i), \quad (3)$$

where $\mathbf{P}(\phi_i, A_j, T_k)$ is the probability for a droplet of size ϕ_i to be detected with an amplitude A_j and a pulse duration T_k. The information about pulse duration makes the system overdetermined, and the correction of spectral broadening is more efficient than it is with the use of the amplitude only.

The transfer matrix has been calculated in three steps. First, the Mie response curve for forward light scattering is used for the calculation of $\mathbf{P}(\phi_i, A_0)$, or probability for a droplet of size ϕ_i to be detected with the amplitude A_0, if it crosses the detection beam in its center, where the incident light intensity is maximum. Second, the coefficient $i_{x,y,z}$, representing the ratio of the light intensity at any location x, y, z in the laser beam to its maximum value at the center, is derived from measurements of the intensity profile in the beam. Finally, the coefficient $\epsilon_{x,y,z}$, representing the percentage of the scattered light collected by the detection diodes, is calculated with a geometrical model of the FSSP optics. With these two coefficients i and ϵ, the pulse generated by a particle crossing the detection beam can be modeled and the measured amplitude can be derived ($A_{x,y,z} = A_0 i_{x,y,z}\epsilon_{x,y,z}$) as a function of the amplitude A_0 that the droplet would produce if it were crossing the center of the beam. The pulse duration is also derived from the comparison of the resulting pulse with the detection threshold. The same model, with the additional constraint of the slit on the front of the detecting diode, provides a simulation of the slit pulse and of the DOF selection. The resulting matrix is represented by $\mathbf{P}(A_0, A_j, T_k)$, which can be calculated for the whole sensitive beam or limited to only the DOF area. The complete transfer matrix is thus equal to

$$\mathbf{P}(\phi_i, A_j, T_k) = \mathbf{P}(\phi_i, A_0)\mathbf{P}(A_0, A_j, T_k). \quad (4)$$

The calculation of the coefficient $i_{x,y,z}$ is similar to the approaches followed by Baumgardner and Spowart (1990) or by Kim and Boatman (1990). The effects of the multiple peaks in the Mie response curve have been analyzed by Dye and Baumgardner (1984) to adjust the values of droplet diameter associated to the size classes in the FSSP, while, with the very fine size resolution of the Fast-FSSP, the Mie peaks are explicitly taken into account in the model. In addition, the light collection efficiency in the detection module ($\epsilon_{x,y,z}$), which is not calculated in previous models because it is not crucial for DOF particles ($\epsilon_{x,y,z} \approx 1$), appears to be very valuable for the numerical calculation of the DOF area and the simulation of coincidence effects. In such calculations, the model must be extended to the whole sensitive beam, and the collection efficiency is essential. Details about the model and the correction procedure are available in Coelho (1996).

Figure 3 shows a comparison of the measured matrices versus the calculated ones for three samples of glass beads, 10–15, 15–25, and 25–35 μm, respectively. The main mode in the distributions is correctly simulated, but significant differences can be noted. The measured distributions show a small percentage of counts with large amplitude and/or large pulse duration. These differences are attributed to coincidences of glass beads whose effects are not represented by the model. This result illustrates a shortcoming in the model validation. On the one hand, one has to use a reference spectrum such as glass beads; on the other hand, it is difficult to reproduce precisely in the laboratory the same conditions as during a flight, especially for the spatial distribution of the particles and their statistics of arrival in the probe sampling volume.

Coincidences involve two or more particles, and the transfer equation becomes nonlinear (in the following equation, the calculation is limited to coincidences of two particles):

$$\mathbf{M}(A_j, T_k) = \sum_i \mathbf{P}(\phi_i, A_j, T_k)\mathbf{f}_a(\phi_i) + \sum_i \sum_l \mathbf{P}^{\text{coinc}}(\phi_i, \phi_l, A_j, T_k)\mathbf{f}_a(\phi_i)\mathbf{f}_a(\phi_l), \quad (5)$$

where $\mathbf{P}^{\text{coinc}}(\phi_i, \phi_l, A_j, T_k)$ is the probability for two particles to be coincident in the beam, with the resulting pulse producing an amplitude A_j and a pulse duration T_k, when the sizes of the coincident particles are ϕ_i and ϕ_l, respectively, and finally for the resulting pulse to be accepted in the DOF (signal amplitude smaller than slit amplitude). Since some particles crossing the beam out-

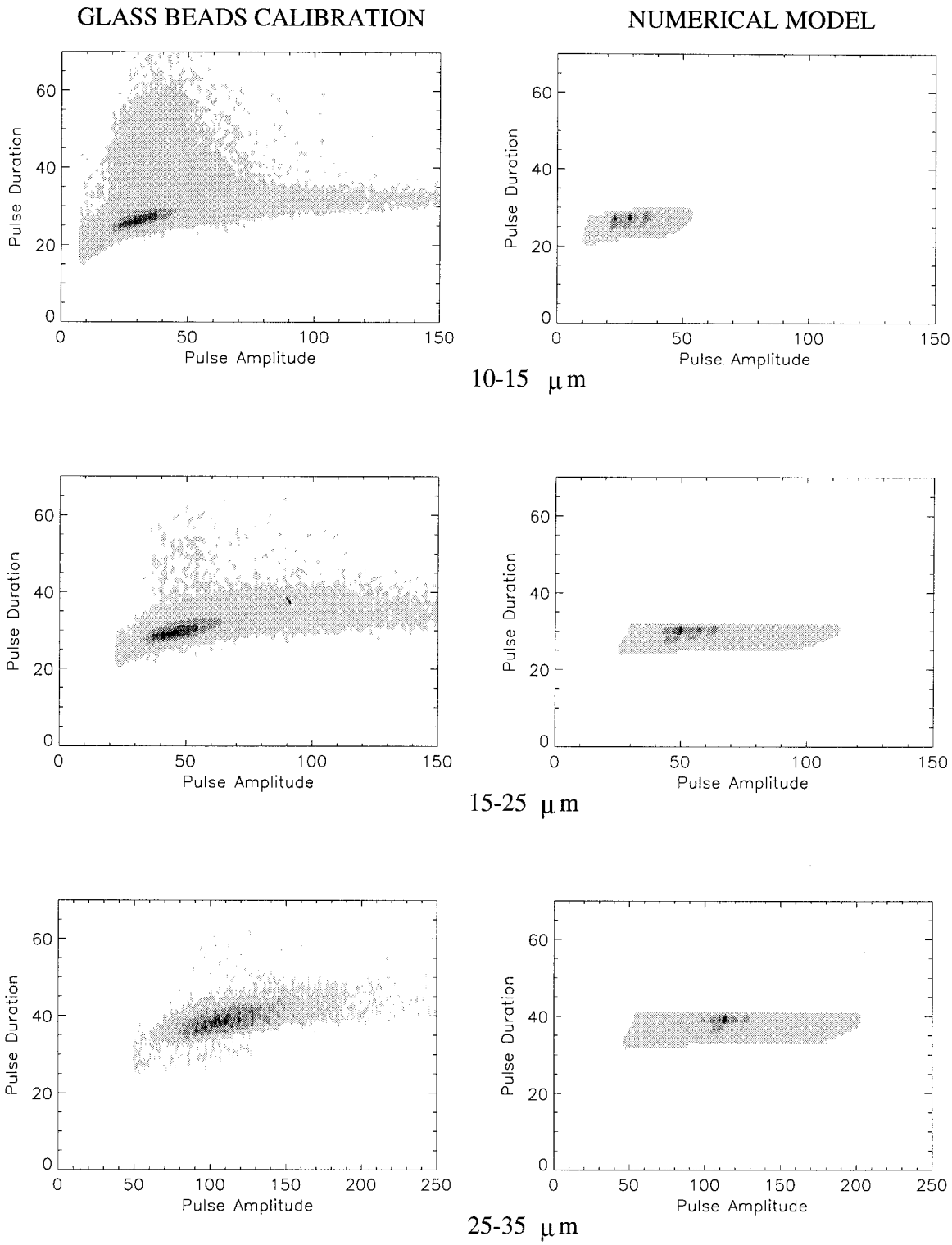

FIG. 3. Matrices of the conditional frequency distributions of pulse duration vs pulse amplitude for three samples of glass beads (10–15, 15–25, and 25–35 μm). The left column shows the measured distributions, and the right column shows the calculated ones.

side of the DOF and coincident with a particle in the DOF are capable of producing a DOF-accepted pulse (Cooper 1988), the calculation must be extended to the whole sensitive beam. This equation is not yet used operationally for correcting coincidence effects because it is computationally too expensive. More efficient numerical solutions are currently being tested at Météo-France.

In summary, the model has been developed for correcting the effects of ambiguities in the Mie curve and beam inhomogeneity. However, it appears that new optics provide a very efficient DOF selection of the particles (Fig. 2) and that the Fast-FSSP spectral broadening due to Mie ambiguities and beam inhomogeneity is no longer significant compared to other sources of spectra broadening, which are not yet taken into account by the model. In particular, the most important broadening effect is due to coincidences when the droplet concentration is larger than 500 cm^{-3}. The model must then be further improved in order to become operational. It has nevertheless been extensively used for analyzing the sensitivity of the measurements to optical settings, particularly for the determination of the optimal DOF area, which is discussed in the next section. The main improvement with respect to the standard probe is the recording of the pulse duration for each particle. This additional parameter provides crucial information about the validity of the detected pulses.

c. Uncertainties in the sampled volume V_s

The sampled volume is the product of the probe sampling section by the particle speed. The value of the particle speed is generally given by the airspeed measured on board the aircraft. However, it has been shown that the particle speed in the sampling tube of the FSSP may be smaller that the true airspeed (Norment 1988). Knowledge of the beam diameter and of the mean pulse duration should allow direct estimation of the particle speed. However, in the standard probe, the activity, or sum of the pulse durations during the sampling period, is not accurate enough for such an estimation. In addition, the mean pulse duration is lengthened by coincidences (Fig. 1b). With the Fast-FSSP that records each pulse duration with a resolution of 1/16 μs, it is possible to build the frequency distribution of the measured pulse durations. In Fig. 2b the value corresponding to particles crossing the beam axis (maximum pulse duration for a single particle) can be precisely estimated at 35 (2.2 μs). Larger values, after the curvature of the distribution changes, are essentially due to coincidences. With a beam diameter of 220 μm, such a value corresponds to a particle speed of 100 m s^{-1}, while the measured airspeed on board the aircraft is 102 m s^{-1}. The uncertainty of this evaluation is still too large to emphasize the difference between the two values. This result is preliminary, and a precise calibration of the procedure is currently under way at Météo-France.

The sampling section is also difficult to characterize precisely. Dye and Baumgardner (1984) and Baumgardner and Spowart (1990) estimate that the dimensions of the cross section cannot be measured to an accuracy better than 15% in the standard probe. In addition, the possible variations of this sampling area as a function of the particle size are not clearly understood. If the laser light is not uniform in the DOF section, small droplets are detected only in the most illuminated region at the center of the DOF, while big particles are detected across the whole DOF area. In the standard probe, where the DOF section includes the beam edge, this effect is significant. The velocity rejection criteria applied to correct the beam edge effects underestimates the small particles with respect to the big ones and leads to an overall uncertainty in the sampling section larger than 20%. For bigger particles, there is also a possibility that the DOF criterion (comparison of signal and annulus pulses in the standard probe, or the signal and slit pulses in the Fast-FSSP) could depend on the particle size. Additional studies will be necessary for clarifying these potential sources of uncertainty.

The main improvement with the Fast-FSSP is the new optical setup, as in the FSSP-300, that provides optical rejection of particles crossing the beam edge. The DOF area can be measured with a 25-μm pinhole in the laboratory to an accuracy better than 10%. Two examples are shown in Fig. 4: a very narrow DOF area and a large one. The uncertainty on the determination of the area with a pinhole is represented by the dotted lines apart from the solid line ($\pm$20 mV in the comparison between signal and slit pulses).

The setting of the DOF is a compromise between statistical significance of the measurements and the sizing accuracy. A small DOF area is more uniform than a large one, but the number of counted particles is also smaller and the statistical significance is reduced. The lower limit for the DOF area is determined by the noise-to-signal ratio of the instrument that affects the comparison of the signal to slit pulses. It results in a narrow region at the border of the DOF where droplets can be indifferently accepted or rejected depending on the random noise of both pulses. This narrow region has a constant area, and it is obvious that the selected DOF area must be large with respect to this undetermined area (Coelho 1996).

Once the size of the DOF area has been selected it is essential to adjust the area of the total sensitive section. The sensitive section is obviously larger than the DOF since particles crossing the edge of the sensitive section are poorly characterized and must be rejected. However, the percentage of coincidences increases exponentially with the sensitive section so that it is important to keep it as small as possible. In the standard probe the ratio of usable to total counts, or the ratio of DOF to sensitive section, is of the order of 10%. With the new optics of the Fast-FSSP, this ratio can be in-

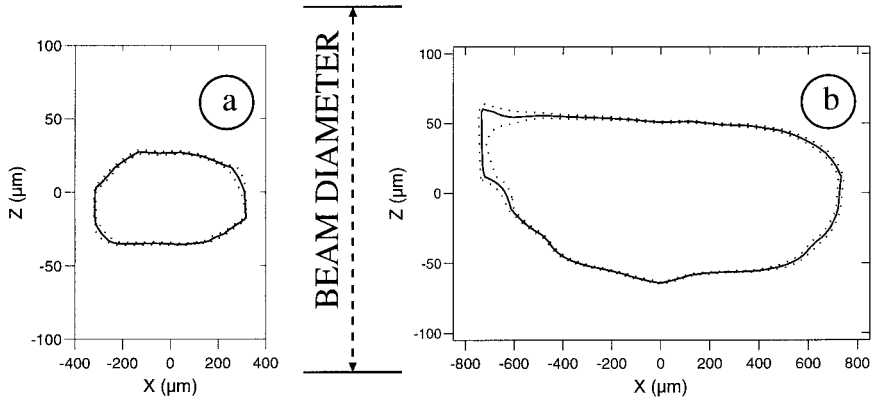

FIG. 4. Examples of DOF areas measured in the laboratory with a 25-μm pinhole: X is along the beam axis, and Z is perpendicular to the beam axis and to the particle trajectory. The dotted lines apart from the solid line correspond to a range of $\pm$20 mV in the comparison between signal and slit pulse amplitudes.

creased to almost 20% with the same DOF area but a reduced sensitive section of the beam.

The Fast-FSSP also provides a way of checking the adequacy of the DOF setting. Three values are recorded for the DOF validation flag, depending on whether the droplet crossed the laser beam inside the DOF, outside the DOF, or at the edge of the DOF (signal pulse smaller, larger, or equal, respectively, to the slit pulse). Figure 8 shows a droplet spectrum measured with the Fast-FSSP. The solid line corresponds to detections validated in the DOF, the dotted line corresponds to the detected particles in the whole sensitive section of the beam, and the dotted–dashed line corresponds to detections that have been validated at the limit of the DOF. The dashed line represents the spectrum measured by the standard FSSP. The difference between the size distribution in the DOF and the distribution without selection shows that the new optics are very efficient at rejecting particles crossing the beam in regions of reduced light intensity (small measured diameters). However, that does not demonstrate that the DOF area is uniform—that is, that there is no significant spectral broadening in the DOF. The laser intensity decreases from the center to the sides of the beam. Therefore, the intensity is minimum at the border of the DOF. Since the two spectra, derived from droplets in the DOF and droplets at the border of the DOF, respectively, are very similar, it can be concluded that the DOF area is well centered and uniform.

Uncertainties due to the time response of the instrument (Baumgardner and Spowart 1990) have not been mentioned because the Fast-FSSP has a bandwidth larger than 2 MHz and a sampling rate of 16 MHz. Therefore, there is no attenuation of the short pulses. Similarly, there is no low-frequency cutoff as in the standard probe, so that long pulses generated at low airspeed are not attenuated either.

d. Uncertainties in the probe calibration

The calibration is the procedure that relates each size class (more precisely the threshold voltage for each class) to a value of droplet diameter. The thresholds are multiples of 1/256 of the maximum voltage, and the sampling is linear. If $I(\phi)$ is the light intensity scattered by a droplet of diameter ϕ and collected by the diode, the measured voltage and the threshold voltages are given by

$$V(\phi) = gI(\phi) + V_0 \quad \text{and}$$

$$V(\phi_i) = i \times V_{\max}/256, \tag{6}$$

where g and V_0 are the gain and the offset of the detection module, respectively. Calibration attempts to determine these two parameters. It is currently performed by using samples of glass beads in the FSSP and further comparing the voltage corresponding to the mode of the measured spectrum to the modal diameter of the glass beads. A correction is necessary because of the difference in refractive index between glass beads and water droplets (Dye and Baumgardner 1984). The accuracy of this procedure is evaluated to about half a class width, that is, $\pm$1.5 μm, mainly due to the spread in the glass beads distribution and the errors in the glass-to-water correction. In addition, the calibration is likely to change during a flight because of vibrations and pollution of the optics by aerosols. Therefore, checking of the probe calibration should be performed before and after each flight. A more accurate calibration can be performed with the droplet generator described in Wendisch et al. (1996), but this apparatus is hardly practicable in the field.

The very fine size resolution of the Fast-FSSP provides an original solution for a self-calibration of the probe with the data collected during a flight. The Mie response curve for forward scattering is characterized by oscillations such that some values of intensity are

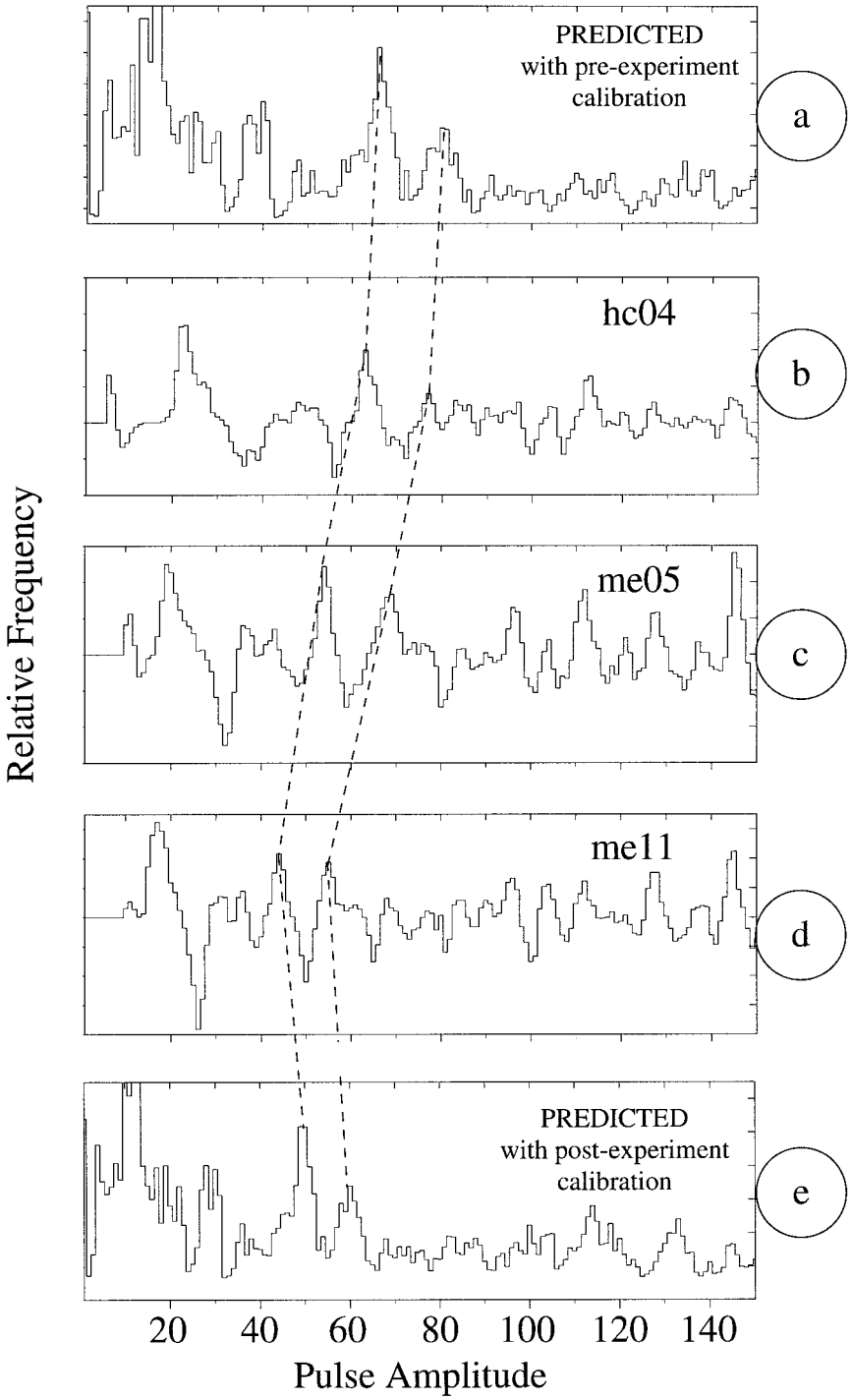

FIG. 5. Probability density function of the measured amplitudes for a uniform size distribution in the Fast-FSSP during the SCMS-95 experiment. (a) Calculated with the numerical model and the calibration coefficients derived from the preexperiment glass beads calibration. (b) Derived from all the spectra measured during the National Center for Atmospheric Research/C130 flight on 22 July 1995. (c) Same as (b) but for the Merlin flight on 4 August 1995. (d) Same as (b) but for the Merlin flight on 10 August 1995. (e) Same as (a) but for coefficients derived from the postexperiment glass beads calibration.

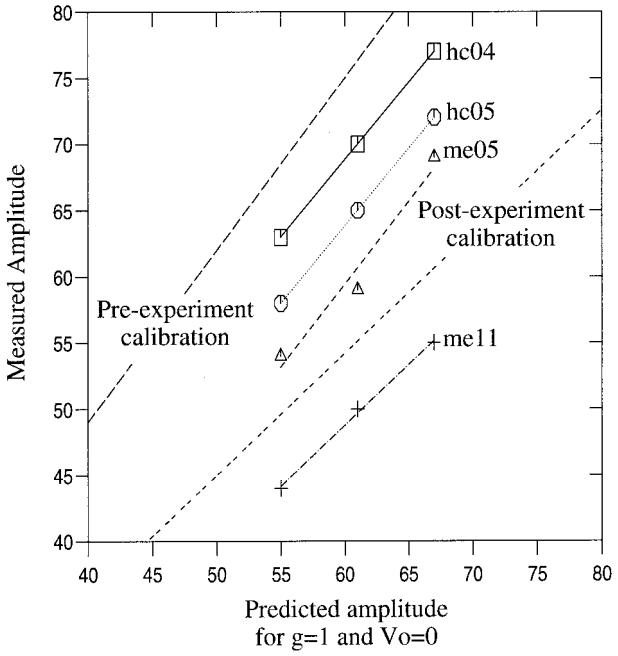

FIG. 6. Comparison of the more frequently measured values of amplitude (identified in Fig. 5) with the values calculated with the numerical model and calibration coefficients of $g = 1$ and $V_0 = 0$.

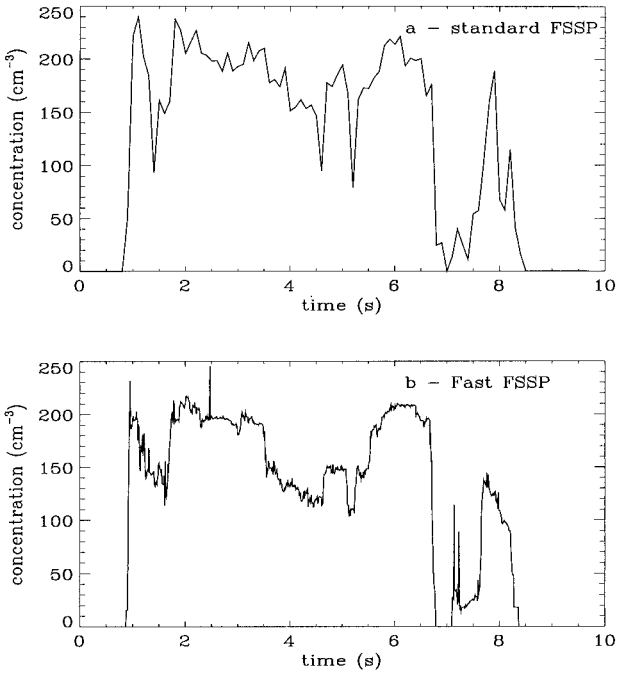

FIG. 7. Time series of the total droplet concentration measured across a cloud cell during the SCMS experiment (Merlin flight 95-11, 1631:40–1631:44 UTC 10 August). (a) Standard FSSP measurements recorded at 10 Hz. (b) Fast-FSSP measurements processed with optimal estimation at a 1-ms time resolution.

more likely to be measured than others (see Fig. 16 in Dye and Baumgardner 1984). The probability density function of the corresponding voltages can be derived by assuming a uniform droplet spectrum and applying the model described in section 4b(2). Peaks can be identified that correspond to fixed values of the droplet diameter. Measured droplet spectra are showing the same peaks superimposed on the actual droplet spectra. By filtering the measured spectra, the peaks can be identified. Averaging a large number of samples is needed for smoothing peaks that are not at fixed voltage values.

This procedure is illustrated in Fig. 5, which represents the probability of counting a given pulse amplitude, as simulated with the model by using the calibration coefficients g and V_0 derived from the preexperiment glass beads calibration (Fig. 5a) and the postexperiment calibration (Fig. 5e). The curves in Figs. 5b–d show the probability of counting derived from measured spectra during the first flight of the Fast-FSSP in SCMS (hc04), the third flight (me05), and the ninth flight (me11). The comparison of the peak voltage values derived from the measured spectra with the peak values obtained with the model (two of those values are connected by dashed lines in Fig. 5) provides the calibration—that is, the values of the gain and the offset during the flight—as shown in Fig. 6. This procedure has been applied on the 10 Fast-FSSP flights of the SCMS-95 experiment. The calibration with the glass beads performed before and after the experiment suggest that the sensitivity of the Fast-FSSP was decreasing significantly throughout the experiment. With the self-calibration procedure it has been possible to determine the calibration coefficients g and V_0 for each flight. Figure 6 shows that the sensitivity decreased progressively from the beginning to the end of the project. The procedure has, however, been limited to the identification of the peaks in the range of amplitudes between 40 and 80 because of a default of linearity of the A/D converter. This default has been corrected now, and better examples of the self-calibration method will be published in the near future.

5. Conclusions

The two following examples illustrate the difference between the standard and the Fast-FSSP. Figure 7 shows the time evolution of the total droplet concentration measured across a convective cloud cell. In Fig. 7a standard FSSP measurements sampled at 10 Hz are shown. At a higher acquisition frequency, random counting noise is superimposed on actual variations of the concentration. In Fig. 7b, Fast-FSSP data have been processed with optimal estimation at a time resolution of 1 ms (Pawlowska et al. 1997). This example demonstrates that sharp transitions in the droplet concentration, such as shown in Brenguier (1993), are common in convective clouds. This phenomenon is crucial for understanding the interaction between turbulence and microphysics. Current acquisition systems, which are cumulating counts in real time, prevent optimal data pro-

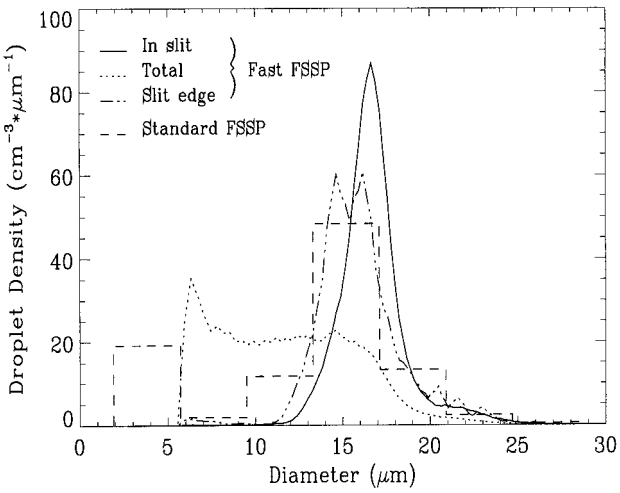

FIG. 8. Droplet size distribution measured in an adiabatic core during the SCMS-95 experiment Merlin flight 95-11, 1631:40–1631:44 UTC 10 August. Solid line: Fast-FSSP DOF-accepted counts. Dotted line: Fast-FSSP total counts. Dashed–dotted line: Fast-FSSP counts selected at the limit of the DOF. Dashed line: Standard FSSP DOF and beam edge selected counts. (The counts in the first class are an instrumental artifact due to the use of the delay mode in the FSSP.)

cessing. It is thus essential to record the complete series of interarrival times with an SPC.

The second example compares the size distributions measured with a standard and a Fast-FSSP (Fig. 8). This cloud section has been selected in an adiabatic core, 400 m above cloud base. The study of spectral broadening has been an active field of research in cloud microphysics. From standard FSSP measurements, it has been suggested that droplet spectra were never as narrow as predicted by the water vapor diffusion theory, even in unmixed cloud updrafts. A firm conclusion has never been reached because of the uncertainty due to the artificial broadening by the instrument. Measurements with the Fast-FSSP are demonstrating that narrow droplet spectra can be observed well above the cloud base (Brenguier and Chaumat 1996). These spectra are not as narrow as predicted, but they are much narrower than previously observed spectra with the FSSP.

The modifications made in the Fast-FSSP are summarized briefly here.

1) Improvement of the DOF optical selection. Optical rejection of particles out of the DOF or crossing the beam edge is much more efficient than the combination of optical and electronic rejection criteria of the standard FSSP. Recording of the DOF selection criterion is also important for validation of the optical setting by comparison of measurements performed in the DOF and at its border (section 4c).
2) Fast electronics. This improvement is obvious if attenuation of the pulse amplitude is to be avoided.
3) No dead time of the electronics. Electronic dead time is a source of counting losses. In addition, it prevents the measurement of interarrival times shorter than the dead time (see item 6 below).
4) Very fine size resolution. From a preliminary analysis of the noise-to-signal ratio in the instrument and the oscillations of the Mie response curve for droplet scattering, it could be concluded that a coarser size resolution would be sufficient. However, both processes are known and their statistics can be taken into account in the transfer function of the instrument. The resulting broadening can thus be corrected statistically but only if the resolution of the measurements is much finer than the final resolution after correction. In addition, if the response curve is not regular, referenced values can be identified in the measured distributions, and a self-calibration procedure, such as described in section 4d, can be developed.
5) Recording of the pulse duration. The pulse duration contains important information about the validity of the detection. A correction procedure based on the conditional transfer matrix of amplitude versus pulse duration is more efficient than a correction based on amplitude only. This is particularly true for correcting coincidence effects whose signature on pulse duration is significant. Pulse duration is also potentially useful for a direct calculation of the particle speed through the counter.
6) Recording of the interarrival time between detections. This crucial parameter is needed for an efficient coincidence correction (section 4a) and for optimal estimation of the droplet concentration at small scales. It is thus essential to record the complete series of time intervals with an adequate resolution.

These improvements are applicable to any SPC. Even item 4, which is specific to size measurements, can be extended to other particle properties. Finally, it must be noted that these improvements become even more beneficial if a similar effort is invested in data processing, such as the transfer matrix of the instrument for correcting spectral broadening and optimal estimation for processing at the smallest scales.

Acknowledgments. The authors acknowledge the support of Météo-France, the University of Wyoming, Department of Atmospheric Sciences, INSU under Grant 95317, and the European Commission under Grant C11∗CT940066.

REFERENCES

Baumgardner, D., 1986: A new technique for the study of cloud microstructure. *J. Atmos. Oceanic Technol.,* **3,** 340–343.

——, and M. Spowart, 1990: Evaluation of the Forward Scattering Spectrometer Probe. Part III: Time response and laser inhomogeneity limitations. *J. Atmos. Oceanic Technol.,* **7,** 666–672.

——, W. Strapp, and J. E. Dye, 1985: Evaluation of the Forward Scattering Spectrometer Probe. Part II: Corrections for coincidence and dead-time losses. *J. Atmos. Oceanic Technol.,* **2,** 626–632.

——, J. E. Dye, and B. W. Gandrud, 1992: Interpretation of measurements made by the Forward Scattering Spectrometer Probe (FSSP-300) during the airborne Arctic stratospheric expedition. *J. Geophys. Res.*, **97,** 8035–8046.

——, B. Baker, and K. Weaver, 1993: A technique for the measurement of cloud structure on centimeters scales. *J. Atmos. Oceanic Technol.*, **10,** 557–565.

Brenguier, J. L., 1989: Coincidence and dead-time corrections for particle counters. Part II: High concentration measurements with an FSSP. *J. Atmos. Oceanic Technol.*, **6,** 585–598.

——, 1993: Observations of cloud microstructure at the centimeter scale. *J. Appl. Meteor.*, **32,** 783–793.

——, and L. Amodei, 1989: Coincidence and dead-time corrections for particle counters. Part I: A general mathematical formalism. *J. Atmos. Oceanic Technol.*, **6,** 575–584.

——, and L. Chaumat, 1996: Condensational droplet growth in cumulus clouds. Preprints, *12th Int. Conf. on Clouds and Precipitation*, Zurich, Switzerland, 57–60.

——, D. Baumgardner, and B. Baker, 1994: A review and discussion of processing algorithms for FSSP concentration measurements. *J. Atmos. Oceanic Technol.*, **11,** 1409–1414.

Coelho, A., 1996: Mesure Aéroportée de la distribution dimensionnelle des gouttelettes d'eau en nuage. Ph.D. thesis, No. 2246, University of Toulouse 151 pp. [Available from Laboratoire Aerologie, OMP, 14, av. E. Belin, 31400 Toulouse, France.]

Cooper, W. A., 1988: Effects of coincidence on measurements with a Forward Scattering Spectrometer Probe. *J. Atmos. Oceanic Technol.*, **5,** 823–832.

Dye, J. E., and D. Baumgardner, 1984: Evaluation of the Forward Scattering Spectrometer Probe. Part I: Electronic and optical studies. *J. Atmos. Oceanic Technol.*, **1,** 329–344.

Kim, Y. J., and J. F. Boatman, 1990: Corrections for the effects of particle trajectory and beam intensity profile on the size spectra of atmospheric aerosols measured with a Forward Scattering Spectrometer Probe. *J. Atmos. Oceanic Technol.*, **7,** 673–680.

Norment, H. G., 1988: Three-dimensional trajectory analysis of two drop sizing instruments: PMS OAP and PMS FSSP. *J. Atmos. Oceanic Technol.*, **5,** 743–756.

Pawlowska, H., J. L. Brenguier, and G. Salut, 1997: Optimal nonlinear estimation for cloud particle measurements. *J. Atmos. Oceanic Technol.*, **14,** 88–104.

Wendisch, M., A. Keil, and A. V. Korolev, 1996: FSSP characterization with monodisperse water droplets. *J. Atmos. Oceanic Technol.*, **13,** 1152–1165.